η_{max}-Charging Strategy for Lithium-Ion Batteries in V2G Applications

Hamzeh Beiranvand
Chair of Power Electronics
Kiel University
Kiel, Germany
hab@tf-uni.kiel.de

Nicola Blasuttigh
Dep. of Engineering and Architecture
University of Trieste
Trieste, Italy
nicola.blasuttigh@phd.units.it

Thiago Pereira
Chair of Power Electronics
Kiel University
Kiel, Germany
tp@tf-uni.kiel.de

Sandra Hansen
Chair of Functional Nanomaterials
Kiel University
Kiel, Germany
sn@tf-uni.kiel.de

Helge Krueger
Chair of Functional Nanomaterials
Kiel University
Kiel, Germany
hkr@tf-uni.kiel.de

Marco Liserre
Chair of Power Electronics
Kiel University
Kiel, Germany
ml@tf-uni.kiel.de

Alessandro Massi Pavan
Dep. of Engineering and Architecture
University of Trieste
Trieste, Italy
apavan@units.it

***Abstract*—The design of charging strategies for lithium-ion (Li-ion) batteries depends on the application. In electric vehicle applications, high charging speed and long battery life are essential requirements. However, with the advent of vehicle-to-grid (V2G) and potential remuneration for electric grid support, maximum user profit could gain increasing interest through efficient operation that also optimizes battery health. Conventional constant-current constant voltage (CCCV) and constant-power constant-voltage (CPCV) charging strategies do not include the optimum efficiency of the battery and charging stations. In this paper, a charging strategy is introduced aiming at maximizing the instantaneous efficiency (η_{max}) of the Li-ion battery and the charging station which minimizes the energy waste. For this purpose, 18650 Li-ion cells and a dual-active-bridge (DAB) converter are considered in the simulations and experimental validations. The results show that the η_{max}-charging strategy outperforms conventional CCCV and CPCV charging strategies in terms of efficiency and material-lifetime compatibility.**

***Index Terms*—Lithium-Ion Battery, Charging Strategy, DAB Converter, Maximum Efficiency, Vehicle to Grid (V2G)**

I. Introduction

The growth of the number of electric vehicles (EVs) not only introduces new challenges on the electrical grid but also brings some advantages and possibilities to stabilize the grid under the significant variability of the energy demand and production [1]. One of the advantages is to utilize EV batteries as distributed energy storage with the so called ancillary services where, in some situations, the profit of the consumer is the priority [2]. Therefore, new battery systems including power electronic converter and battery pack shall be developed targeting the aforementioned objectives.

From the hardware point of view, building blocks of battery systems (i.e. power semiconductors and battery cells) require different thermal operating conditions and using the same package challenges the design of battery packs [3]. Nonetheless, battery current can be controlled to a pre-defined reference overtime (or different state of charges, SOCs) using suitable control software which is mainly referred as charging strategy or charging protocol [4].

The existing charging strategies are mainly developed considering cell performance improvements. Since a battery is a complex system of chemo-physical phenomena, its charging strategy can be impacted by multiple factors such as:

- Cell stack shape [5]
- Material composition of electrodes, separator, and electrolyte [6],
- Electro-thermal quantities [7], [8]
- Battery manufacturing processes [9]
- Mechanical stresses [10], [11]

These are the motivations for many of existing charging strategies [12] which lead to a gradual improvement in battery lifetime. The direct impact of charging strategy on the lithium ion batteries is very well identified in the literature [13]. However, a battery system is made of numerous cells and power electronic converters and it is not clear that if such charging strategies could lead to an optimum performance for battery systems. Charging strategies for battery packs comprising of multiple cells also might be different from that of a single cell [14], [15]. These studies do not consider power losses of fast charging stations which influences the overall

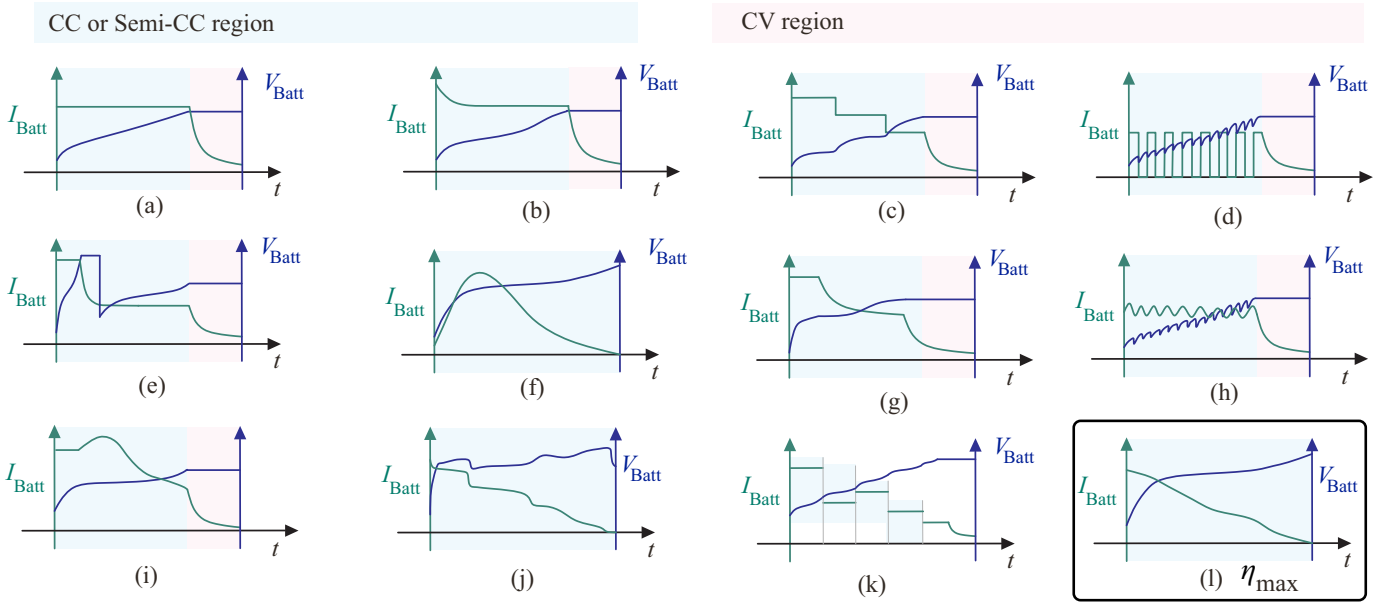

Fig. 1. Charge strategies of Li-ion Batteries: (a) CCCV [16], (b) CPCV [17], (c) Multistep CCCV [18], (d) Pulse charging [19], (e) Boost Charging [20], (f) universal voltage protocol (UVP) [21], (g) Constant temperature constant voltage (CTCV) [22] , (h) AC-ripple charging [23], (i) constant incremental capacity dQ/dV [24], (j) MPC [25], (k) six-step 10-minute (6S-10M) charging strategy based on machine learning [26], and (l) proposed η_{max}.

efficiency of the system.

Power electronic converters are different for grid integration of EV charging station. Type of the upstream grid, AC or DC could also impact on the power electronic converter topology [27], [28]. State-of-the-art charging strategies are rarely designed for maximizing the profit by minimizing the energy losses [16]. Round-trip efficiency of the Li-ion battery storage system and its interface power electronic converters for grid applications are studied in [29]. Authors of [30] have optimized the round-trip efficiency of a 50 kW charging station. A similar study on an unidirectional on-board EV charger reveals the possibility to save more than 40% energy losses in entire 12kWh battery and 3.3 kW power converter system [31]. However, the power converters are based on the full-bridge topology and cannot be used in V2G applications where power flow is bidirectional. In [32], charger losses are added to the battery losses aiming at minimizing the total losses using a dynamic programming algorithm. However, a commercial DC source is utilized as the charger where the topology of the converter and operational details are not provided. Therefore, the applicability of the results for V2G application remains questionable. Results of a study on the system level energy losses analysis in [33] shows that the total energy losses could be decreased if adaptive charging current is selected in an optimization process. Nonetheless, the charging current evolution is not sufficiently elaborated versus the state of charge (SOC) as an index of material compatibility for fast charging strategies. Therefore, the existing gap in the energy efficient charging strategies shall be addressed.

This paper proposes η_{max}-charging strategy for V2G applications where EVs are directly interfaced to an LV grid through a bidirectional dual active bridge (DAB) converter. Comprehensive analysis is performed to identify the optimal efficiency characteristics of the DAB Li-ion battery system. Simulations are carried out on a 20 kW 800V DAB converter at the interface of a 20 kWh battery pack. Simulation and experiments' results show that the current profile is compatible with material charge limitations while the efficiency is preserved at maximum instantaneous value and higher than CCCV/CPCV methods.

This paper is organized in five sections. Section II gives a brief overview of charging strategies. The proposed charging strategy is explained in section III and experimentally validated in section IV. Conclusions are given in section V.

II. Charging Strategies Driving Mechanism

Charging strategies are implemented in a battery system through a controller. Therefore, charging strategies have been categorized regarding the control strategy as none-feedback-based, feedback-based, and intelligent methods [36]. Conventional charge strategies such as CCCV are usually adopted because of the simplicity of the controller where an internal current control loop could provide a robust operation of the power converter [37]. In another classification, charging strategies are regarded as passive and active methods. Usually, in passive or none-feedback-based methods, the charging strategy is implemented based on measurable parameters, i.e. voltage, current, and temperature. While, in active methods, the charging strategy control reference is adapted to the status of the battery desired states. There is a significant literature on the charging strategies/protocols for lithium ion batteries that it can be found in [12], [36]–[38].

A charging strategy can be designed to serve an specific control objective. These protocols can be compared disregarding the type, active or passive methods. Indexes such as

power converter hardware requirement, control and modeling complexity, impact on the battery lifetime, usability in fast charging, energy efficiency, and safety might be used to compare these charging strategies quantitatively and qualitatively. Table I summarizes some of the charging strategies in the literature.

Charging strategies such as CCCV and CPCV (see Fig. 1 (a) and (b)) are targeting simplicity both in control and modeling and therefore a minimal hardware requirements owing to constant or nearly constant current profile over the power semiconductors. To establish a meaningful comparison, CCCV and CPCV are considered as the reference and other methods are qualitatively compared. Lifetime, speed, efficiency, and safety are set to "0" for CCCV and CPCV methods.

Multi-step charging strategy applies an staircase decreasing overtime as shown in Fig. 1 (c) and therefore high charging speeds can be achieved [18]. Since a high amount of current is applied to the cell in a short time, the safety and lifetime of the cell degrades in comparison to CCCV. Moreover, the charging station requires switches with higher current ratings.

Pulse charging is based on considering a rest time for batteries after a time interval of charging with a constant current [19], [34]. Pulse charging is shown in Fig. 1 (d). The main drawback is hardware implementation, control and modeling, while it can improves the battery cell lifetime and better safety indices due to controlled temperature during the rest time.

Constant temperature constant voltage (CTCV) charging strategy, depicted in Fig. 1 (g), has been enabled through a classical proportional-integral-derivative (PID) controller in [22]. 20% faster charging speed in comparison to CCCV can be guaranteed utilizing this method. Since the temperature of battery cells are directly controlled, high level of safety is expected.

AC current ripple charging strategies, shown in Fig. 1 (h), deal with the variable impedance of the battery [23], [35]. The hypothesis is to apply an AC content to current to charge the battery at the minimum impedance resulting in the minimum energy losses. In one hand, the methodology leads to increased complexity in the hardware of the power converter. On other hand, the positive impact of this kind of charge strategies is not strongly verified [39].

A group of charging strategies formulate the charge process as an optimization problem and try to minimize the impacts from side reactions while tying to increase the speed of charge [25], [40]–[43]. Optimal control techniques such as model predictive control (MPC) and electrochemical models such as single particle model are dominating in these methods. Main advantage is to directly act on the lifetime indicators of the batteries at electrochemical level. An example charging profile is illustrated in Fig. 1 (j).

Machine learning tools simplify the control and modeling at the cost of increased need for data and data analysis. Machine learning tools can be included in all the aforementioned charging strategies to boost their performance. For example, machine learning is applied to multi-step charging strategies resulting in significant performance improvement, in particular for fast charging purposes in [26]. A 6-step charging strategy has been developed which is able to charge the cell to 80% SOC in 10-minute (6S-10M). Beside all the advantages, it needs higher computational effort for training or to connected to database and consequently higher hardware requirement. Due to high speed, i.e. high current level at near zero SOC, the semiconductor current is overrated in comparison to a normal CCCV method.

There is a tremendous literature on charging strategies each targeting an objective which can be studied an compared, similarly. Table I summarizes a comparison including some other strategies such as boost charging [20], universal voltage profile (UVP) [21], and constant incremental capacity dQ/dV [24] which are shown in Fig. 1 (e), (f), and (i), respectively.

The development of charging strategies capable of controlling electrochemistry of batteries optimally enables highly reliable and safe batteries at the cost of increased cost of modeling and control complexity while the interfacing hardware converter does not need significant modification [44], [45]. The capacity of active materials for absorbing charge decreases at high current densities which imposes an operation restriction for batteries [46]. Most of the charging strategies, shown in Fig. 1, fail their compatibility to material physical limits in

TABLE I
QUALITATIVE COMPARISON OF THE WELL-KNOWN CHARGING STRATEGIES.

Index	**Reference**	**Method**	**Converter**	**Control**	**Modeling**	**Lifetime**	**Speed**	**Efficiency**	**Safety**
a	[16]	CCCV	++	+	++	0	0	0	0
b	[17]	CPCV	++	+	++	0	0	0	0
c	[18]	Multistep CCCV	+	+	+	−−	++	+	−−
d	[19], [34]	Pule Charging	−−	−	−−	++	++	+	+
e	[20]	Boost Charging	+	+	0	+	++	+	+
f	[21]	UVP	++	++	+	+	+	+	+
g	[22]	CTCV	++	+	++	0	+	+	++
h	[23], [35]	AC-ripple Charging	−−	−−	−	−	0	0	−
i	[24]	Constant dQ/dV	++	0	0	+	++	+	+
j	[25]	MPC (Optimal Control)	−	0	−−	+	0	+	+
k	[26]	Machine Learning	−−	+	−	0	++	+	−
l	This paper	Proposed η_{max}	++	++	+	+	+	+	+

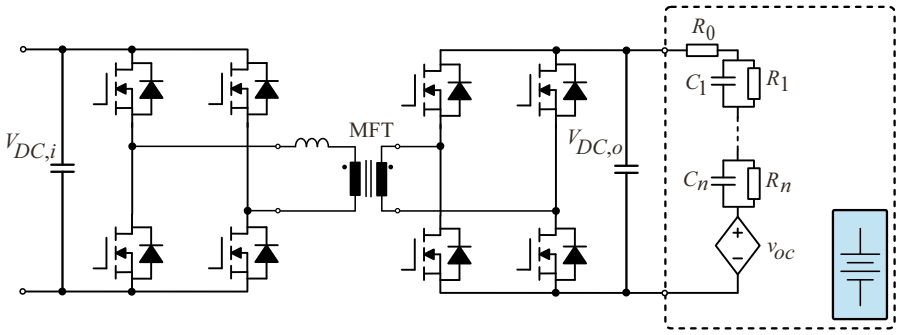

Fig. 2. Battery system consisting of a DC fast charger (DAB converter) and a battery pack composed of serial and parallel connected cells.

handling the current density. Thereby, this paper elaborates a charge strategy which improves the efficiency performance of the cell without increased complexity in the control and modeling and hardware requirements.

III. Proposed η_{max}-Charging Strategy

This section describes η_{max}-charging strategy where the instantaneous efficiency of the system including DAB converter and battery pack is minimized at each SOC. For this reason, a comprehensive losses estimation of both components is also analysed. Fig. 2 shows the battery system under study.

A. DAB Converter Losses

DAB converter losses can be split into semiconductor and transformer losses. The former comprise conduction and switching losses while the latter include both windings and magnetic core losses.

Power losses of the semiconductors can be averaged over the fundamental operating frequency of a power converter [47]–[49]. In DAB, fundamental operating frequency is equal to the switching frequency, f_{sw}, of the semiconductors. In this work, parasitic parameter losses such as the output capacitance C_{OSS} is neglected from the calculations as the switching frequencies is low, i.e. 20 kHz. The conduction losses of a single semiconductor device can be computed as [48]:

$$P_{cond} = f_{sw} \int_0^{\frac{1}{f_{sw}}} v_{ON}\big(i_D(\xi), T_j\big) \cdot i_D(\xi)\, d\xi \qquad (1)$$

where i_D is the current through the device, v_{ON} is the voltage of the semiconductor during the conduction, and T_j is the junction temperature of the semiconductor.

Switching losses calculation strongly depends on other nearby parasitic elements. Switching losses in the DAB primary side H-Bridge can be disregarded if soft-switching operations are achieved. On the other hand, when voltage changes during the battery pack's charge/discharge cycle, operating points for the secondary side can be found outside the soft-switching range. A relatively accurate estimation of the switching losses can be written as follows [49]:

$$P_{sw} \approx \Big(E_{on}\big(V_{DC}, i_D, T_j\big) + E_{off}\big(V_{DC}, i_D, T_j\big)\Big) f_{sw} \qquad (2)$$

where E_{on} and E_{off} are switching energy losses during on and off commutation and V_{DC} is the voltage stress over the semiconductor in off state.

Medium frequency transformers (MFTs), if optimally designed, might dissipate approximately 0.5% of the overall converter losses. Neglecting the parasitic parameter losses, copper and core losses can be used for estimating its efficiency. Due to the behavior of high frequency waveforms, copper losses are calculated using the well-known Dowell's equation, which takes into account the proximity and skin effect in the transformer windings. In particular, the total copper losses $P_{Cu,loss}$ can be computed as:

$$P_{Cu,loss} = I_{RMS}^2 \cdot \big(R_{ac,p} + R_{ac,s} \cdot n_T^2\big) \qquad (3)$$

where I_{RMS} is the transformer RMS current for each specific operating point, $R_{ac,p}$ and $R_{ac,s}$ are the primary and secondary transformer AC resistance, respectively, and n_T is the transformer ratio.

The so-called AC resistance factor is used to determine the primary and secondary winding resistances [50], which can be computed as:

$$\begin{aligned} F_{R_x} &= R_{ac,x}/R_{dc,x} = \\ &= A\left(\frac{sinh(2A)+sin(2A)}{cosh(2A)-cos(2A)} + \right. \\ &\left. + \left[\frac{2(N_x^2-1)}{3}\right]\frac{sinh(A)+sin(A)}{cosh(A)-cos(A)}\right) \end{aligned} \qquad (4)$$

where $A = d_f/\delta$ is the winding conductor thickness normalised with respect to the conductor skin depth, N_x is the number of winding layers and $R_{dc,x}$ is the DC winding resistance where x denotes the primary or secondary winding.

The magnetic flux density within the transformer core and the core materials affect core losses. Due to the non-sinusoidal nature of the primary and secondary voltages, as well as the flux density, it is necessary to compute losses using the Improved Generalized Steinmetz Equation (iGSE) [51] rather than the original Steinmetz Equation (OSE). If the trapezoidal waveform of the flux density $B(t)$ for single-phase shift (SPS) modulation is considered, its maximum value decreases as the phase shift increases and its derivative cancels at the instants where the voltages have opposite values as described in

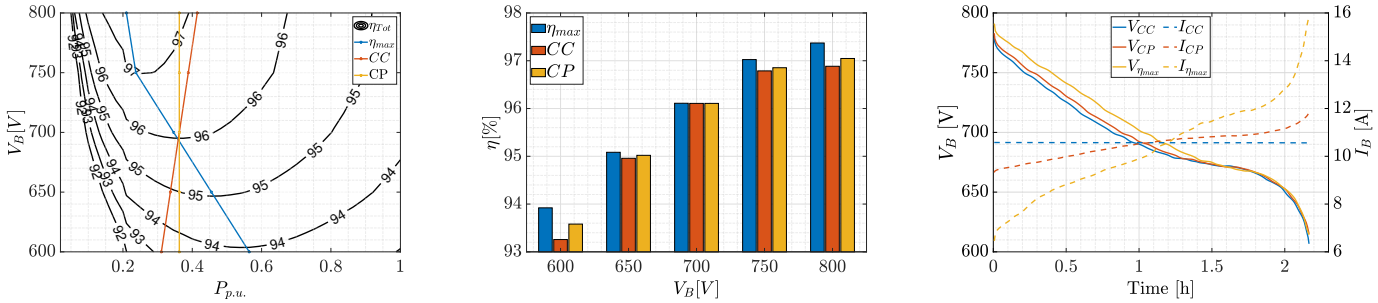

(a) (b) (c)

Fig. 3. Representation of η_{max}, CCV and CPCV strategies in discharging process of the battery system: (a) battery system efficiency map showing the existence of the optimum point, (b) comparing the efficiency results at different voltages (SOCs), and (c) current and voltage profile at battery pack terminals.

[52]. Considering the soft ferrite magnetic material properties considered in this work, the core losses are calculated as:

$$P_{Core,loss} = \frac{k_i}{\pi}(2B_m)^{\beta-\alpha}\left(\frac{V_{DC,i}}{2NA_c}\right)^{\alpha} \cdot [\varphi|d-1|^{\alpha} + (\pi-\varphi)(d+1)^{\alpha}] \quad (5)$$

where A_c is the cross section area of the core column, V_i the input voltage, N is the primary winding turns number, $d = n_T V_{DC,o}/V_{DC,i}$ is the dc conversion ratio and φ the phase-shift angle. The constant parameters k_i, α and β are obtained by the core material datasheet.

B. Battery Losses

Typically, battery losses can be split in different contributions such as ohmic, reversible and irreversible reaction losses. Different dynamic cell models with different complexity and accuracy have been used and published [53], [54]. However, circuit-oriented models, in addition to mathematical and electrochemical ones, have high potential in terms of accuracy, parametrization and usefulness. The terminal behavior of the battery can be described by a series of RC-pairs where the power losses can be estimated by internal resistance values and current measurements. In this work, a model with three RC cells in series with an inductance and a resistance are used as suggested in [55]. Parameters estimation techniques are applied to derive the RC time constant values dynamically. Therefore, battery losses is directly calculated from the estimated parameters.

The battery losses are calculated by adding the Joule's losses as follows:

$$P_{bat,loss} = P_{cell,loss} \cdot N_{tot} = R_{bat,eq} \cdot i_o^2 = = \sum_{j=0}^{3} R_j \cdot \frac{N_{sc}}{N_{ps}} \cdot i_o^2 \quad (6)$$

where R_j is the j-th resistive element, i_o is the total battery current, N_{sc} is the number of series cells, N_{ps} is the number of parallel strings, $R_{bat,eq}$ is the equivalent battery pack resistance and $N_{tot} = N_{sc} \cdot N_{ps}$ is the total number of cells.

Temperature, SOC and C-rate are the main parameters that cause internal battery pack resistance. For this reason, a good estimation method for battery resistance during operations is mandatory in order to estimate power losses. In this work, the existence of an internal management system typically called the Battery Management System (BMS) is assumed which, in addition to providing the battery SOC, also estimates its internal impedance during the operation. Several techniques can be used for online estimation of the internal battery impedance as a function of temperature and SOC [56]–[58].

C. η_{max}-Charging Strategy Implementation

The analysis given in this paper is valid for a DAB converter configuration constructed from the results of a design optimization process. In a DAB converter with power design optimization, the power losses could be significant both in power semiconductors or MFT. Therefore, as an initial step, a design optimization is carried out to achieve an optimum combination of the semiconductors and magnetic components.

To evaluate the converter and battery system energy efficiency, the converter voltage at battery side is varied from 600 to 800 V and the battery current from 0 to the rated power of the converter. Total calculated efficiency of the DAB converter and a 20 kWh battery are shown in Fig. 3 (a). As it can be seen from figure, for each voltage level (i.e. SoC) there is a unique optimum point and, since the behavior is convex, the optimum point can be tracked using a local search algorithm.

The optimum points respectively determine the η_{max}-charging strategy control commands as in Fig. 3 (b). The charging strategy is the result of a compromise between converter losses and the battery losses. Utilizing this charge strategy in a DAB converter with high losses might push the battery system toward higher losses and negatively impact on the battery lifetime.

η_{max}-charge strategy presents superior performance in term of energy losses in a full cycle charging in comparison to CCCV and CPCV charging strategies. Moreover, the achieved current profile, Fig. 3 (c), is inline with the material physical limits as a function of SOC therefore extended lifetime is also expected.

The implementation of η_{max}-charging strategy is straightforward. Fig. 4 illustrates the implementation of the proposed η_{max}-charge strategy in the DAB converter controller. The

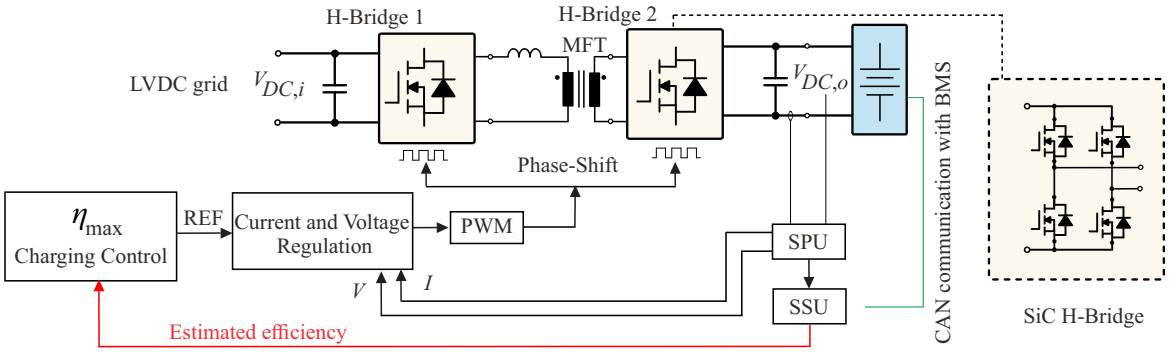

Fig. 4. The charging station under study with an integrated η_{max}-charging strategy. Reference current control is obtained through the efficiency estimation method and maximum efficiency tracking algorithm.

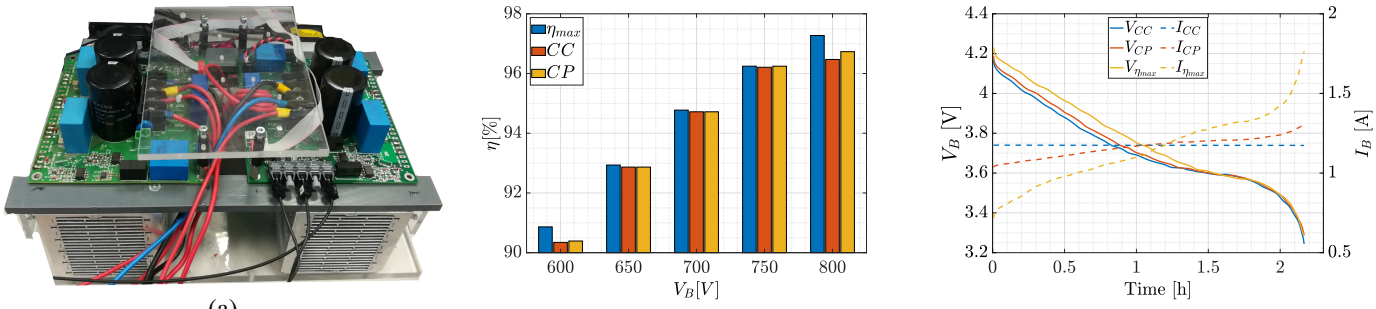

(a) (b) (c)

Fig. 5. Experiment results for η_{max}, CCCV and CPCV charging strategies in discharging process of the battery system: (a) DAB converter photograph of the 800 V 10 kW DAB Converter unit, (b) Measured efficiencies, and (c) single-cell current and voltage charging profiles.

efficiency of the DAB converter can be measured directly from the measured DC voltage and currents from grid and battery side. The efficiency of the battery pack can be estimated from the the parameters delivered by battery management system (BMS). A simple proportional integral (PI) controller is used to control the current or voltage to a reference set point which as routine in the field of power electronics. The outer loop which is responsible for the maximum efficiency tracking is much more slower than the inner current control loop. Therefore, computationally efficient maximum efficiency tracking points can be easily implemented. The details of the algorithm used in this paper is the topic of the next publication related to this project.

IV. Experimental Verification

To correctly validate the proposed method a DAB converter is build using optimum solutions and presented analysis in the previous section. Moreover, the operation of the converter tuned to achieve soft switching during the commutation of the SiC power semiconductors. The implemented DAB converter ensures the correctness of the experiments as it is expected from the analytical analysis. A 10 kW DAB converter is realized which can be scaled to high powers by paralleling sufficient number of 10 kW units. A photograph of the built DAB converter is depicted in Fig. 5 (a). To simplify the test procedure and save time, two 10kW bidirectional DC sources (EA-PSB 9750-40 3U), are used to emulate the behavior of the grid and also the battery. The efficiency of the converter can be easily measured by a power analyzer form the DC ports. Power analyzer YOKGAWA WT1800 is used in the experiments of this paper. Battery cell tester, Biologic VSP3e is utilized for characterizing 18650 cells. The internal loop current controller and the outer loop maximum efficiency tracking algorithm are implemented in the dSPACE SCALEXO environment. Switching frequency of the converter is 20kHz and physical RC filters are used to cancel the measurement noises at the input of the dSPACE ADCs.

The starting point for the experiments is the battery emulation. Dynamic stress tests are performed to validate the equivalent circuit parameters of the battery. Considering that a lithium ion terminal voltage varies from 2.6 to 4.2 V from 0 to 100% SOC, the battery pack voltage will vary between 500 to 800 V where 191 cell are connected in series. The dynamics of battery is emulated using a bidirectional source so both charging and discharging modes can be studied. Input voltage of the converter was fixed at 800 V and the secondary side to the battery pack emulators. Therefore the converter and battery efficiencies can be experimentally measured at different discrete SOCs or over a continuous variation of voltage profile.

Fig. 5 (b) shows the measured efficiencies of the DAB converter and battery pack at 5 different SOCs, i.e. battery pack voltage set $V_S \in \{600V, 650V, 700V, 750V, 800V\}$. This figure demonstrates that the proposed method is able to

maintain the highest efficiency for the converter in comparison to CCCV and CPCV methods. In particular when the battery is at very low or very high SOCs, the proposed η_{max}-charging strategy shows superior performance as expected from the numerical simulations. Fig. 5 (c) shows the current and voltage profiles for a single cell inside the battery pack. The current profile decreases monotonously as the battery SOC increase and vice versa. This behavior is similar to multistep charging strategies suitable for fast charging stations. Therefore, it can be concluded that the proposed method is materiel compatible and not only can be used for V2G application but also for fast charging purposes. The obtained experimental results confirm the correctness of the conducted numerical studies in previous section. η_{max}-charging strategy saves more than 1% losses, particularly at very high and low SOCs in comparison to CCCV and CPCV charging strategies which is a significant improvement.

V. Conclusion

The Li-ion battery voltage is a function of SOC and impacts the efficiency of the power electronics converters. Thereby, a charging strategy based on the instantaneous maximum efficiency of dual-active-bridge (DAB) converter and battery (η_{max}) is proposed in this paper to minimize energy waste, particularly in V2G applications. Preliminary simulation and experiment results show that η_{max}-charging strategy saves more than 1% power losses in comparison to CCCV and CPCV charging strategy in a charge/discharge of the battery. Moreover, the current profile imposes less stress on the material by modifying the current density as a function of SOC.

Acknowledgement

This work was supported in party by Gesellschaft für Energie und Klimaschutz Schleswig-Holstein (EKSH) within the framework of the project "Doppelt Schnell Doppelt Sicher (DSDS)" (Number: 8/12-39) and in part funded by the European Union - European Regional Development Fund (EFRE), the German Federal Government and the State of Schleswig-Holstein (Number: LPW-E/1.1.2/1486).

References

[1] N. B. Arias, S. Hashemi, P. B. Andersen, C. Træholt, and R. Romero, "Distribution system services provided by electric vehicles: recent status, challenges, and future prospects," *IEEE Transactions on Intelligent Transportation Systems*, vol. 20, no. 12, pp. 4277–4296, 2019.

[2] S. Esmailirad, A. Ghiasian, and A. Rabiee, "An extended m/m/k/k queueing model to analyze the profit of a multiservice electric vehicle charging station," *IEEE Transactions on Vehicular Technology*, vol. 70, no. 4, pp. 3007–3016, 2021.

[3] Y. Li and Y. Han, "A module-integrated distributed battery energy storage and management system," *IEEE Transactions on Power Electronics*, vol. 31, no. 12, pp. 8260–8270, 2016.

[4] P. Keil and A. Jossen, "Charging protocols for lithium-ion batteries and their impact on cycle life—an experimental study with different 18650 high-power cells," *Journal of Energy Storage*, vol. 6, pp. 125–141, 2016.

[5] G. Zhang, C. E. Shaffer, C.-Y. Wang, and C. D. Rahn, "Effects of non-uniform current distribution on energy density of li-ion cells," *Journal of The Electrochemical Society*, vol. 160, no. 11, p. A2299, 2013.

[6] M. R. Palacín, "Understanding ageing in li-ion batteries: a chemical issue," *Chemical Society Reviews*, vol. 47, no. 13, pp. 4924–4933, 2018.

[7] M. Xu, R. Wang, P. Zhao, and X. Wang, "Fast charging optimization for lithium-ion batteries based on dynamic programming algorithm and electrochemical-thermal-capacity fade coupled model," *Journal of Power Sources*, vol. 438, p. 227015, 2019.

[8] H. Perez, S. Dey, X. Hu, and S. Moura, "Optimal charging of li-ion batteries via a single particle model with electrolyte and thermal dynamics," *Journal of The Electrochemical Society*, vol. 164, no. 7, p. A1679, 2017.

[9] Y. Liu, R. Zhang, J. Wang, and Y. Wang, "Current and future lithium-ion battery manufacturing," *IScience*, vol. 24, no. 4, p. 102332, 2021.

[10] K. Zhang, Y. Zhang, J. Zhou, Y. Li, B. Zheng, F. Yang, and Y. Kai, "A stress-based charging protocol for silicon anode in lithium-ion battery: Theoretical and experimental studies," *Journal of Energy Storage*, vol. 32, p. 101765, 2020.

[11] B. Lu, Y. Zhao, Y. Song, and J. Zhang, "Stress-limited fast charging methods with time-varying current in lithium-ion batteries," *Electrochimica Acta*, vol. 288, pp. 144–152, 2018.

[12] A. Tomaszewska, Z. Chu, X. Feng, S. O'kane, X. Liu, J. Chen, C. Ji, E. Endler, R. Li, L. Liu *et al.*, "Lithium-ion battery fast charging: A review," *ETransportation*, vol. 1, p. 100011, 2019.

[13] S. S. Zhang, "The effect of the charging protocol on the cycle life of a li-ion battery," *Journal of power sources*, vol. 161, no. 2, pp. 1385–1391, 2006.

[14] Q. Ouyang, Z. Wang, K. Liu, G. Xu, and Y. Li, "Optimal charging control for lithium-ion battery packs: A distributed average tracking approach," *IEEE Transactions on Industrial Informatics*, vol. 16, no. 5, pp. 3430–3438, 2019.

[15] Y. Li, K. Li, Y. Xie, B. Liu, J. Liu, J. Zheng, and W. Li, "Optimization of charging strategy for lithium-ion battery packs based on complete battery pack model," *Journal of Energy Storage*, vol. 37, p. 102466, 2021.

[16] Y. Gao, X. Zhang, Q. Cheng, B. Guo, and J. Yang, "Classification and review of the charging strategies for commercial lithium-ion batteries," *IEEE Access*, vol. 7, pp. 43 511–43 524, 2019.

[17] U. S. Kim, J. Yi, C. B. Shin, T. Han, and S. Park, "Modeling the thermal behaviors of a lithium-ion battery during constant-power discharge and charge operations," *Journal of The Electrochemical Society*, vol. 160, no. 6, p. A990, 2013.

[18] Y.-H. Liu, C.-H. Hsieh, and Y.-F. Luo, "Search for an optimal five-step charging pattern for li-ion batteries using consecutive orthogonal arrays," *IEEE Transactions on Energy Conversion*, vol. 26, no. 2, pp. 654–661, 2011.

[19] X. Huang, Y. Li, A. B. Acharya, X. Sui, J. Meng, R. Teodorescu, and D.-I. Stroe, "A review of pulsed current technique for lithium-ion batteries," *Energies*, vol. 13, no. 10, p. 2458, 2020.

[20] P. H. Notten, J. O. het Veld, and J. Van Beek, "Boostcharging li-ion batteries: A challenging new charging concept," *Journal of Power Sources*, vol. 145, no. 1, pp. 89–94, 2005.

[21] Z. Guo, B. Y. Liaw, X. Qiu, L. Gao, and C. Zhang, "Optimal charging method for lithium ion batteries using a universal voltage protocol accommodating aging," *Journal of Power Sources*, vol. 274, pp. 957–964, 2015.

[22] L. Patnaik, A. Praneeth, and S. S. Williamson, "A closed-loop constant-temperature constant-voltage charging technique to reduce charge time of lithium-ion batteries," *IEEE Transactions on Industrial Electronics*, vol. 66, no. 2, pp. 1059–1067, 2018.

[23] L.-R. Chen, S.-L. Wu, T.-R. Chen, W.-R. Yang, C.-S. Wang, and P.-C. Chen, "Detecting of optimal li-ion battery charging frequency by using ac impedance technique," in *2009 4th IEEE Conference on Industrial Electronics and Applications*. IEEE, 2009, pp. 3378–3381.

[24] L. Lao, S. Wu, and Q. Zhang, "Optimized fast charging protocol for cylindrical lithium-ion battery based on constant incremental capacity algorithm," *International Journal of Energy Research*, vol. 45, no. 2, pp. 2222–2230, 2021.

[25] C. Zou, X. Hu, Z. Wei, T. Wik, and B. Egardt, "Electrochemical estimation and control for lithium-ion battery health-aware fast charging," *IEEE Transactions on Industrial Electronics*, vol. 65, no. 8, pp. 6635–6645, 2017.

[26] P. M. Attia, A. Grover, N. Jin, K. A. Severson, T. M. Markov, Y.-H. Liao, M. H. Chen, B. Cheong, N. Perkins, Z. Yang *et al.*, "Closed-loop optimization of fast-charging protocols for batteries with machine learning," *Nature*, vol. 578, no. 7795, pp. 397–402, 2020.

[27] G. Wang, G. Konstantinou, C. D. Townsend, J. Pou, S. Vazquez, G. D. Demetriades, and V. G. Agelidis, "A review of power electronics for

grid connection of utility-scale battery energy storage systems," *IEEE Transactions on Sustainable Energy*, vol. 7, no. 4, pp. 1778–1790, 2016.

[28] A. Poorfakhraei, M. Narimani, and A. Emadi, "A review of multilevel inverter topologies in electric vehicles: Current status and future trends," *IEEE Open Journal of Power Electronics*, vol. 2, pp. 155–170, 2021.

[29] M. Schimpe, M. Naumann, N. Truong, H. C. Hesse, S. Santhanagopalan, A. Saxon, and A. Jossen, "Energy efficiency evaluation of a stationary lithium-ion battery container storage system via electro-thermal modeling and detailed component analysis," *Applied energy*, vol. 210, pp. 211–229, 2018.

[30] D. Lyu, T. B. Soeiro, and P. Bauer, "Impacts of different charging strategies on the electric vehicle battery charger circuit using phase-shift full-bridge converter," in *2021 IEEE 19th International Power Electronics and Motion Control Conference (PEMC)*. IEEE, 2021, pp. 256–263.

[31] N. Kim, J.-H. Ahn, D.-H. Kim, and B.-K. Lee, "Adaptive loss reduction charging strategy considering variation of internal impedance of lithium-ion polymer batteries in electric vehicle charging systems," in *2016 IEEE Applied Power Electronics Conference and Exposition (APEC)*. IEEE, 2016, pp. 1273–1279.

[32] Z. Chen, B. Xia, C. C. Mi, and R. Xiong, "Loss-minimization-based charging strategy for lithium-ion battery," *IEEE Transactions on Industry Applications*, vol. 51, no. 5, pp. 4121–4129, 2015.

[33] Y. Ding, H. Wu, Z. Gao, and H. Zhang, "An adaptive charging strategy of lithium-ion battery for loss reduction with thermal effect consideration," in *2021 IEEE 1st International Power Electronics and Application Symposium (PEAS)*. IEEE, 2021, pp. 1–7.

[34] S. Li, Q. Wu, D. Zhang, Z. Liu, Y. He, Z. L. Wang, and C. Sun, "Effects of pulse charging on the performances of lithium-ion batteries," *Nano Energy*, vol. 56, pp. 555–562, 2019.

[35] L.-R. Chen, S.-L. Wu, D.-T. Shieh, and T.-R. Chen, "Sinusoidal-ripple-current charging strategy and optimal charging frequency study for li-ion batteries," *IEEE Transactions on Industrial Electronics*, vol. 60, no. 1, pp. 88–97, 2012.

[36] N. Ghaeminezhad and M. Monfared, "Charging control strategies for lithium-ion battery packs: Review and recent developments," *IET Power Electronics*, vol. 15, no. 5, pp. 349–367, 2022.

[37] J. Wu, X. Li, S. Zhou, S. Hu, and H. Chen, "Constant-current, constant-voltage operation of a dual-bridge resonant converter: Modulation, design and experimental results," *Applied Sciences*, vol. 11, no. 24, p. 12143, 2021.

[38] Y. Parvini, A. Vahidi, and S. A. Fayazi, "Heuristic versus optimal charging of supercapacitors, lithium-ion, and lead-acid batteries: An efficiency point of view," *IEEE Transactions on Control Systems Technology*, vol. 26, no. 1, pp. 167–180, 2017.

[39] M. J. Brand, M. H. Hofmann, S. S. Schuster, P. Keil, and A. Jossen, "The influence of current ripples on the lifetime of lithium-ion batteries," *IEEE Transactions on Vehicular Technology*, vol. 67, no. 11, pp. 10 438–10 445, 2018.

[40] X. Hu, Y. Zheng, X. Lin, and Y. Xie, "Optimal multistage charging of nca/graphite lithium-ion batteries based on electrothermal-aging dynamics," *IEEE Transactions on Transportation Electrification*, vol. 6, no. 2, pp. 427–438, 2020.

[41] Q. Ouyang, J. Chen, J. Zheng, and H. Fang, "Optimal multiobjective charging for lithium-ion battery packs: A hierarchical control approach," *IEEE Transactions on Industrial Informatics*, vol. 14, no. 9, pp. 4243–4253, 2018.

[42] Y. Gao, X. Zhang, B. Guo, C. Zhu, J. Wiedemann, L. Wang, and J. Cao, "Health-aware multiobjective optimal charging strategy with

[46] C. Heubner, M. Schneider, and A. Michaelis, "Diffusion-limited c-rate: a fundamental principle quantifying the intrinsic limits of li-ion batteries," *Advanced Energy Materials*, vol. 10, no. 2, p. 1902523, 2020.

coupled electrochemical-thermal-aging model for lithium-ion battery," *IEEE Transactions on Industrial Informatics*, vol. 16, no. 5, pp. 3417–3429, 2019.

[43] X. Lin, X. Hao, Z. Liu, and W. Jia, "Health conscious fast charging of li-ion batteries via a single particle model with aging mechanisms," *Journal of Power Sources*, vol. 400, pp. 305–316, 2018.

[44] U. R. Koleti, T. N. M. Bui, T. Q. Dinh, and J. Marco, "The development of optimal charging protocols for lithium-ion batteries to reduce lithium plating," *Journal of Energy Storage*, vol. 39, p. 102573, 2021.

[45] C.-H. Lee, Z.-Y. Wu, S.-H. Hsu, and J.-A. Jiang, "Cycle life study of li-ion batteries with an aging-level-based charging method," *IEEE Transactions on Energy Conversion*, vol. 35, no. 3, pp. 1475–1484, 2020.

[47] L. F. Costa, G. Buticchi, and M. Liserre, "Optimum design of a multiple-active-bridge dc–dc converter for smart transformer," *IEEE Transactions on Power Electronics*, vol. 33, no. 12, pp. 10 112–10 121, 2018.

[48] T. Pereira, F. Hoffmann, and M. Liserre, "Performance evaluation of the multi-winding redundancy approach in mtb dc-dc converters," in *2021 IEEE Energy Conversion Congress and Exposition (ECCE)*. IEEE, 2021, pp. 3599–3606.

[49] L. Camurca, T. Pereira, F. Hoffmann, and M. Liserre, "Analysis, limitations and opportunities of modular multilevel converter-based architectures in fast charging stations infrastructures," *IEEE Transactions on Power Electronics*, 2022.

[50] H. Beiranvand, E. Rokrok, and M. Liserre, "*Vf* -constrained $\eta\rho$ -pareto optimisation of medium frequency transformers in ISOP-DAB converters," *IET Power Electronics*, vol. 13, no. 10, pp. 1984–1994, Aug. 2020.

[51] K. Venkatachalam, C. R. Sullivan, T. Abdallah, and H. Tacca, "Accurate prediction of ferrite core loss with nonsinusoidal waveforms using only steinmetz parameters," in *2002 IEEE Workshop on Computers in Power Electronics, 2002. Proceedings.* IEEE, 2002, pp. 36–41.

[52] N. Fritz, M. Rashed, S. Bozhko, F. Cuomo, and P. Wheeler, "Analytical modelling and power density optimisation of a single phase dual active bridge for aircraft application," *The Journal of Engineering*, pp. 3671–3676, 2019.

[53] M. Chen and G. A. Rincon-Mora, "Accurate electrical battery model capable of predicting runtime and IV performance," *IEEE transactions on energy conversion*, vol. 21, no. 2, pp. 504–511, 2006, publisher: IEEE.

[54] B.-A. Enache, E. Lefter, and C. Stoica, "Comparative study for generic battery models used for electric vehicles," May 2013, pp. 1–6.

[55] A. Kersten, "Modular Battery Systems for Electric Vehicles based on Multilevel Inverter Topologies - Opportunities and Challenges," Ph.D. dissertation, 2021.

[56] O. Theliander, A. Kersten, M. Kuder, W. Han, E. Grunditz, and T. Thiringer, "Battery Modeling and Parameter Extraction for Drive Cycle Loss Evaluation of a Modular Battery System for Vehicles Based on a Cascaded H-Bridge Multilevel Inverter," *IEEE Transactions on Industry Applications*, vol. 56, Sep. 2020.

[57] Y. Zheng, M. Ouyang, X. Han, L. Lu, and J. Li, "Investigating the error sources of the online state of charge estimation methods for lithium-ion batteries in electric vehicles," *Journal of Power Sources*, vol. 377, pp. 161–188, Feb. 2018.

[58] M. Kuipers, P. Schröer, T. Nemeth, H. Zappen, A. Blömeke, and D. U. Sauer, "An Algorithm for an Online Electrochemical Impedance Spectroscopy and Battery Parameter Estimation: Development, Verification and Validation," *Journal of Energy Storage*, vol. 30, p. 101517, Aug. 2020.